Clarifying Hydrogeological Structure of Deep Catastrophic Landslide Using Airborne Electromagnetic Survey, Spatial Patterns of Stream Flow and Drilling Investigation

Hiromitsu ISSHIKI[1*], Atsuhiko KINOSHITA[1], Teruyoshi TAKAHARA[1], Tadanori ISHIZUKA[1], Ken'ichirou KOSUGI[2], Ryo SAKAI[3], Makoto OYAMA[4], Shinji KOMATSU[5], Yuji UEHARA[5], Masami ITOU[5], Makoto YAMANE[5], Katsushi KAWATO[6] and Minoru OKUMURA[6]

[1] Public Works Research Institute (1-6 Minamihara, Tsukuba-shi, Ibaraki 3058516, Japan)

[2] Graduate School of Agriculture Kyoto University (Kitashirakawa, Oiwake-cho, Sakyo-ku, Kyoto, Kyoto 6068502 , Japan)

[3] MLIT kii-santi Sabo Office (1681 Sanzai-cho, Gojyo-shi, Nara, 6370002, Japan)

[4] Kinki Regional Development Bureau (1-5-44 ootemae, Chuou-ku, osaka 5508586, Japan)

[5] OYO Corporation (7 Kanda-Mitoshiro-cho, Chiyoda-Ku, Tokyo 1018486, Japan)

[6] Nippon engineering consultants co, Ltd (3-23-1 Komagome, Toshima-ku, Tokyo 1700003, Japan)

*Corresponding author. E-mail: isshiki-hiromitu@oyonet.oyo.co.jp

Deep catastrophic landslides (DCLs) were caused due to rainfall by Typhoon Talas struck the Kii Peninsula in September 2011. From the fact that the severe flood has been recorded in 1889 and 1953, there is no doubt that DCLs occurs at a high frequency in the Kii Peninsula. Therefore, extraction of the slope with fear of DCL is an urgent issue. In this study, we intended for the Kitamata district where the DCL occurred, and clarified geological structure by drilling investigation and surface exploration. Next, we estimated the hydrogeological structure which is restricted by the fault, by measuring the flow rate of each basin and calculating the specific discharge distribution. Then, in comparison with the resistivity obtained from the airborne electromagnetic survey, it is revealed that there is very relevant to the resistivity distribution and the hydrogeological structure.

Key words: deep catastrophic landslide, hydrogeology, fault, airborne electromagnetic survey, resistivity

1. INTRODUCTION

Heavy rains of typhoon Talas caused deep catastrophic landslides (DCLs), debris flow, and river flooding in parts of the Kii Peninsula in September 2011. More than 50 DCLs have occurred and a large number of people were affected in Nara Prefecture. From the fact that DCLs had occurred in the Kii Peninsula in 1889 and in 1953, there is no doubt that DCL occurs at a high frequency in the district. Therefore, extraction of the slope with fear of DCL is an urgent issue.

About the extracting method of the slope with fear of the DCL, many studies have been accomplished until now. *Sasahara et al.* [2014] have studied the slope with fear of DCL by focusing on terrain deformed by creep edifice using LiDAR data. *Chigira et al.* [2012] explain that there are small cliffs on the upper slope before the occurrence of DCLs; small cliffs were formed by gravitational deformation of the slope. *Yokoyama et al.* [2012] studied the technique of extracting the creep slope by analyzing the DEM data. These studies were based on an analysis technique that focuses on the topography of the ground surface. There are few studies focused on the subsurface structure which has influenced outbreak of the DCL.

In this study, we performed geological survey to

clarify the geological distribution, structures and weathering conditions of rocks in Kitamata district. Next, we measured the flow rate of each catchment around the survey area for calculation of specific discharge distribution. And we performed airborne electromagnetic survey to estimate the hydrogeological structure and geological structure. The relations between that information were discussed.

2. INVESTIGATIVE METHOD

2.1 Geological distribution and structure

We performed geological survey for the entire landslide to clarify the geological distribution, structures and weathering conditions of rocks in Kitamata district. Geological survey was carried out uniformly not only within the landslide but also around back slope and valley. We observed the outcrops along the route, and measured the fault direction, weathering conditions and geological structure. In order to obtain underground information, we have conducted boring surveys. Three drilling surveys were carried out on the main course of traverse in a collapse place, four on the subcourse of traverse, four on a non-collapsing background, and three on the collapse sediment. Moreover, using the drilling hole, a borehole scope observation and the permeability test were carried out and groundwater level was measured. As a result, we created a geological cross-section and geological plan in and around the collapse site.

2.2 Hydrogeological structure

In order to understand the hydrological environment over a wide area including a landslide, we measured the flow rate of each catchment around the survey area. In A River, we measured the flow rate at 4 points in the main stream and 18 points in the tributaries, in B River at 1 point in the main stream and 6 points in the tributaries, in C River at 5 points in the main stream and 11 points in the tributaries. We were confirmed a spring situation of the slope in further. We have conducted measurement from 9 to 10 November and 6 to 7 December 2012. Specific discharge was calculated dividing the observed flow rate by the catchment area to obtain the information about groundwater distribution around the area. The area of a catchment, the measured flow, and the calculated specific discharge are shown in **Table 1**.

Table 1 Summary of catchment area, flow rate and specific discharge

division		measure point	catchmennt area (km^2)	2012/11/9～10 flow rate (L/s)	2012/11/9～10 specific discharge ($L/s/km^2$)	2012/12/6～7 flow rate (L/s)	2012/12/6～7 specific discharge ($L/s/km^2$)
A River	main	A-1	0.551	–	–	–	–
	main	A-2	0.471	6.1	12.9	7.5	15.9
	main	A-3	0.320	9.7	30.2	12.0	37.3
	tributary	A-4	0.160	3.6	22.3	4.1	25.7
	tributary	a-1	0.006	0.00	0.5	1.0	168.3
	tributary	a-2	0.008	0.01	1.3	0.02	2.5
	tributary	a-3	0.003	0.00	0.0	0.00	0.0
	tributary	a-4	0.005	0.03	6.0	0.03	6.0
	tributary	a-5	0.005	0.1	10.0	0.1	16.0
	tributary	a-6	0.009	–	–	0.1	5.6
	tributary	a-7	0.015	0.1	3.3	0.1	8.7
	spring	a-7-1	–	0.00		0.00	
	tributary	a-8	0.018	0.1	2.8	0.2	8.9
	spring	a-8-1	–	0.04	–	0.01	–
	tributary	a-9	0.012	0.03	2.5	0.1	10.0
	spring	a-9-1	–	0.02	–	0.03	–
	tributary	a-10	0.032	0.3	9.4	0.5	15.0
	spring	a-10-1	–	0.07	–	0.05	–
	tributary	a-11	0.034	0.4	11.8	0.5	15.6
	spring	a-11-1	–	0.05	–	0.02	–
	tributary	a-12	0.021	0.3	12.4	0.4	18.6
	tributary	a-13	0.043	0.7	17.0	0.9	21.6
	tributary	a-14	0.092	2.7	29.7	3.4	37.0
	tributary	a-15	0.017	0.1	7.6	0.2	13.5
	tributary	a-16	0.032	0.6	17.5	0.8	23.4
	tributary	a-17	0.012	0.02	1.7	0.03	2.5
	tributary	a-18	0.010	0.01	1.0	0.00	0.0
B River	main	B-1	0.079	0.4	5.2	0.5	6.3
	tributary	b-1	0.009	0.00	0.0	0.0	0.0
	tributary	b-2	0.011	0.01	0.9	0.3	27.3
	tributary	b-3	0.006	0.01	1.7	0.2	33.3
	tributary	b-4	0.006	0.1	11.7	0.1	16.7
	tributary	b-5	0.012	0.1	5.8	0.1	10.0
	spring	b-5-1	–	0.01	–	0.00	–
	tributary	b-6	0.004	0.0	0.0	0.00	0.0
C River	main	C-1	0.954	20.4	21.4	20.1	21.1
	main	C-2	0.607	17.1	28.2	19.9	32.8
	main	C-3	0.225	4.6	20.6	7.2	32.0
	main	C-4	0.305	0.02	0.1	0.02	0.1
	main	C-5	0.076	0.9	11.6	1.3	17.5
	tributary	c-1	0.007	0.1	14.3	0.1	12.9
	tributary	c-2	0.01	0.00	0.0	0.00	0.0
	tributary	c-3	0.008	0.1	8.8	0.1	11.3
	tributary	c-4	0.006	0.02	3.3	0.04	6.7
	tributary	c-5	0.015	0.00	0.0	0.00	0.0
	tributary	c-6	0.019	0.9	44.7	0.9	48.4
	tributary	c-7	0.021	0.7	31.4	0.4	18.6
	tributary	c-8	0.025	0.6	23.6	0.9	34.4
	tributary	c-9	0.017	0.3	17.6	0.4	23.5
	tributary	c-10	0.045	2.6	57.8	2.7	60.0
	tributary	c-11	0.023	0.3	11.7	0.3	13.5

2.3 Airborne electromagnetic survey

Airborne electromagnetic survey can estimate underground specific resistivity structure by measuring the induced secondary magnetic field generated by the effect of subsurface geology. This secondary magnetic field is induced after applying electromagnetic waves generated by transmitter either from the air or ground surface. Generally, airborne electromagnetic survey is carried out by using helicopter. A bird containing transceiver is towed with a constant speed and maintaining the terrain clearance.

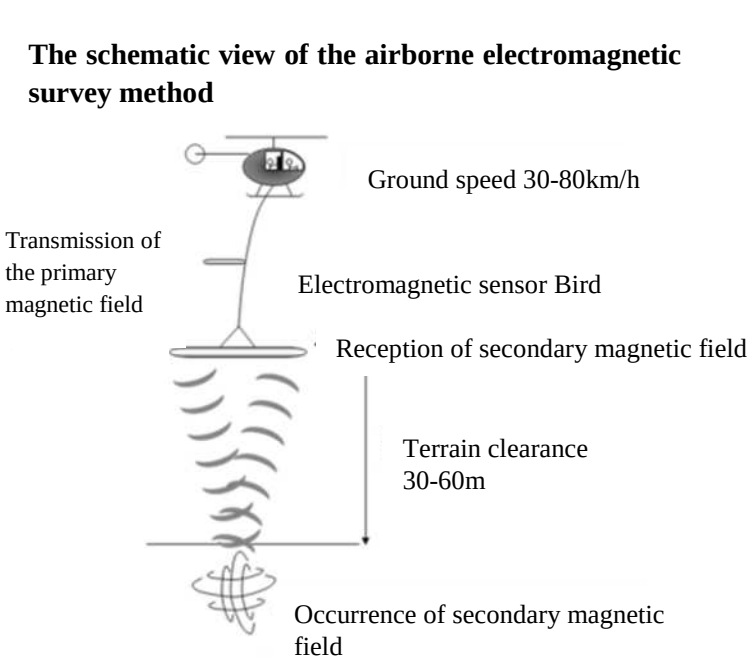

Fig.1 The schematic view of the airborne electromagnetic survey method

Fig. 1 shows the schematic view of the airborne electromagnetic survey method with actual survey situation. With this system, it is possible to explore about 100 to 150 m depth and measure three dimensional resistivity distributions by navigating a helicopter in a lenticular pattern.

Resistivity obtained by airborne electromagnetic survey is a value that varies depending on the type of rock, water saturation, porosity, and clay minerals. Generally, resistivity is high in fresh hard rock, and decreases with the degree of weathering (*Archie* [1942], *Takakura* [2009]). Weathering tends to be relatively high with increasing the porosity by the development of cracks. Besides, if the groundwater level of the slope is low the specific resistivity becomes higher; the trend is opposite in the case of high groundwater level. We performed airborne electromagnetic survey for the target area of about 4km^2, including slope of the DCL.

3. RESULT AND DISCUSSION

3.1 Occurrence of deep catastrophic landslide

In Kitamata district, the scale of the DCL was 170m in width, 370m in length and about 50m in maximum depth. Amount of landslide sediment was estimated at 1.3 million m^3. Landslide sediment has flowed out and formed a natural dam. Part of the sediment reached to Kitamata River and swept away 4 houses. **Fig. 2** shows the gradient map based on the DEM data before and after the collapse. The collapse was generated involving flat surface of a ridge, according to the inclined view before the collapse. DCL has occurred in the convex slope above the two small tributaries and the catchment area is almost same as the collapsed area. According to the LiDAR topographic map and aerial photographs before the collapse, clear linear depressions are seen in the summit area and creep terrains are seen on the slope. We can guess that the slope had been gradually deformed by gravity.

3.2 Geological structure of the surveyed area

A geological map of area near collapse is shown in **Fig. 3** and an estimated geological cross-section in **Fig. 6**. Slope inclination before the collapse is around 35° and gentler than other DCLs that occurred by Typhoon Talas at the same period. For example, the slope of the Nagatono district and Akadani district shows 40°. DCL has occurred along the ridge in the east-southeast to west-northwest direction where F-1 fault with south-facing scarp is distributed and head scarp of the DCL was formed there. It is very loose around the F-1 fault and mineral veins are developed. In addition, F-2 fault is distributed on the west side of the collapse in the north-south direction.

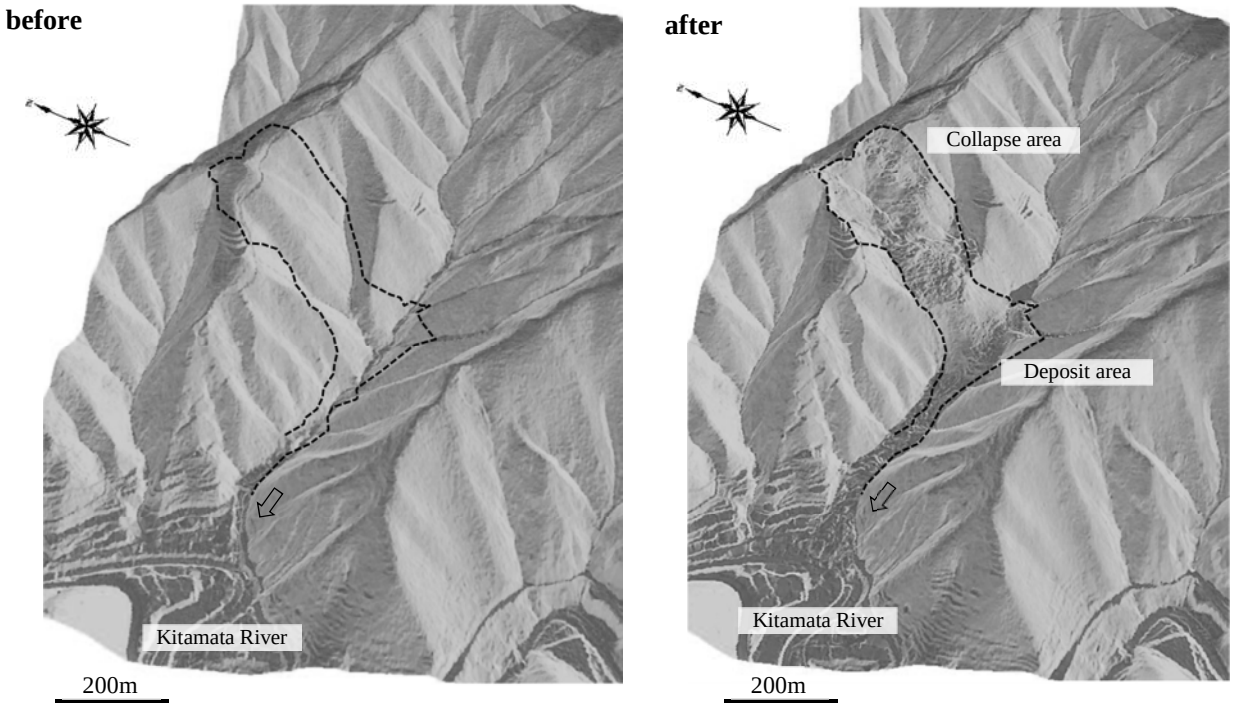

Fig.2 Bird's-eye view of before and after the collapse

It has been confirmed by drilling survey that collapse soil mass is made up gravel-like portion composed of breccia set which was completely loosened and massive portion made of a strongly weathered rock which remains mesh of cracks. Thickness of the weathered mass layer is 50m. Because fresh rock was not found, it is estimated that progress of weathering reached to the deep layer around the collapsed surface before the occurrence of DCL. Weathered rock is widely distributed along the scarp of the collapse. Tephra which was identified about 7,300 years old remains on the flat surface of the ridge. It is estimated that DCL occurred in the area where no significant topographical change in the period after the tephra covered terrain surface.

The bedrock geology of the landslide indicates that the predominant sandstone layer and mud mixed layer corresponding to Shimanto Belt Yukawa layer is distributed in alternate layers. Schistosity plane and bedding planes of these are repeatedly folded slightly along the fold axis of N20° ~ 30° W in general and it shows structure of outfacing dip locally. However, the angle between collapsed surface and boundary layer of sandstone dominant and pelitic mixed rock is 20° to 40°. It is said that DCL occurred on the infacing dip in macro scale shown as the cross section in **Fig. 6**. It is contemplated that strongly weathered bed rock has remained, which could have lost by outcrop of surface material such as shallow slope failure in case it would be dip slope. It is estimated that the DCL in Kitamata district has been regulated by the geological structure predisposition mentioned above and as following.

3.3 Geological structure for regulating the flow of water

As shown in **Fig. 3**, catchment area including the DCL is only slightly larger than the area of the collapse. But, spring water is frequently observed immediately after the collapse from the steep cliff which is formed by DCL. It was assumed that occurrence of inflow of groundwater from outside the basin. According to geological survey, sandstone layers are found along the ridge. It is about 30 degree north slope, and it forms infacing dip. And the layers are cut by F-1 fault in the south slope and distributed in wedge-shaped, cut by F-1 fault in the south slope (**Fig. 4**). This wedge shaped sandstone is distributed continuously along the ridge and it make easy that the groundwater from the high- altitude area flows into the DCL site (**Fig. 6**).

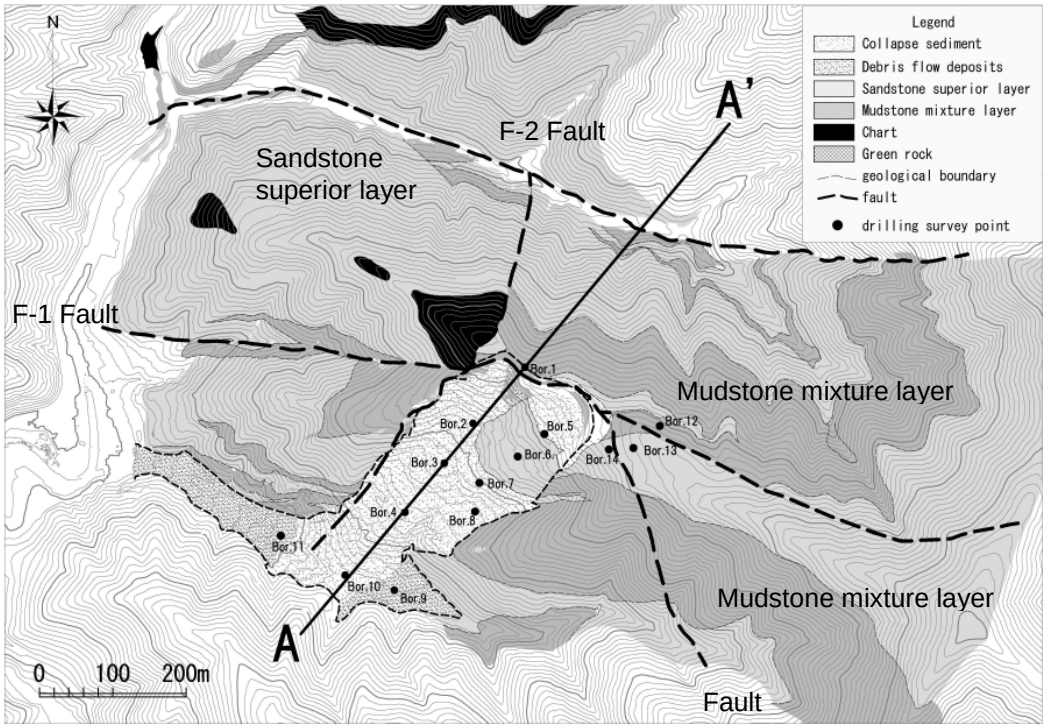

Fig.3 Geological map

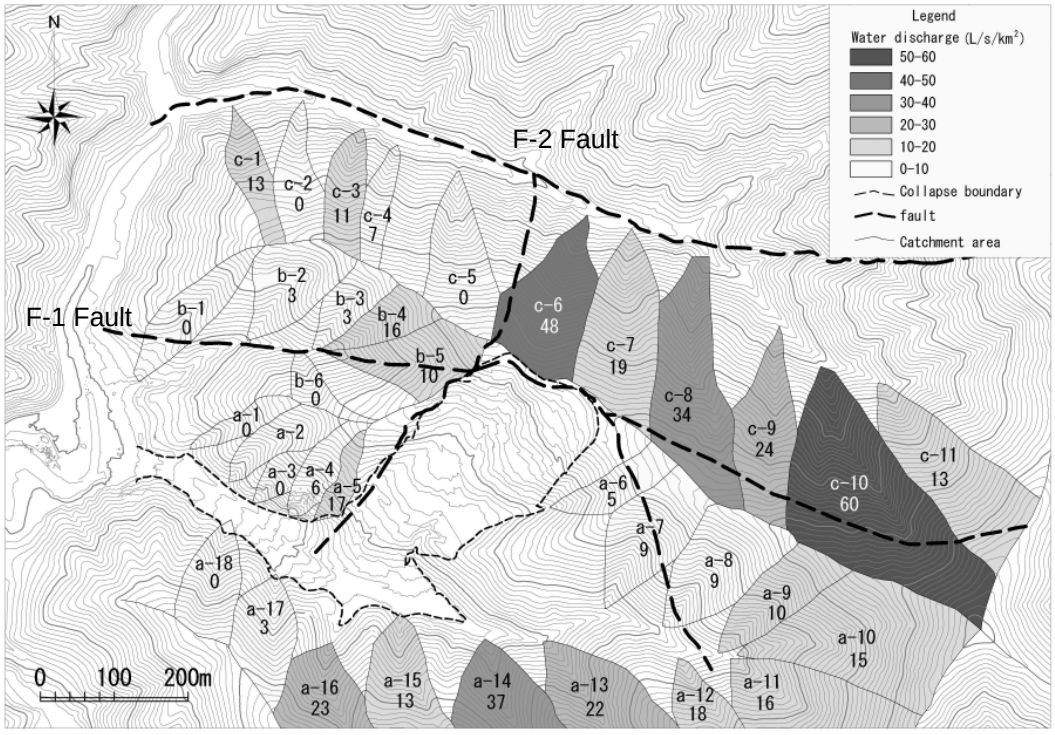

Fig.4 Specific discharge distribution map (Measured on December, 2012)

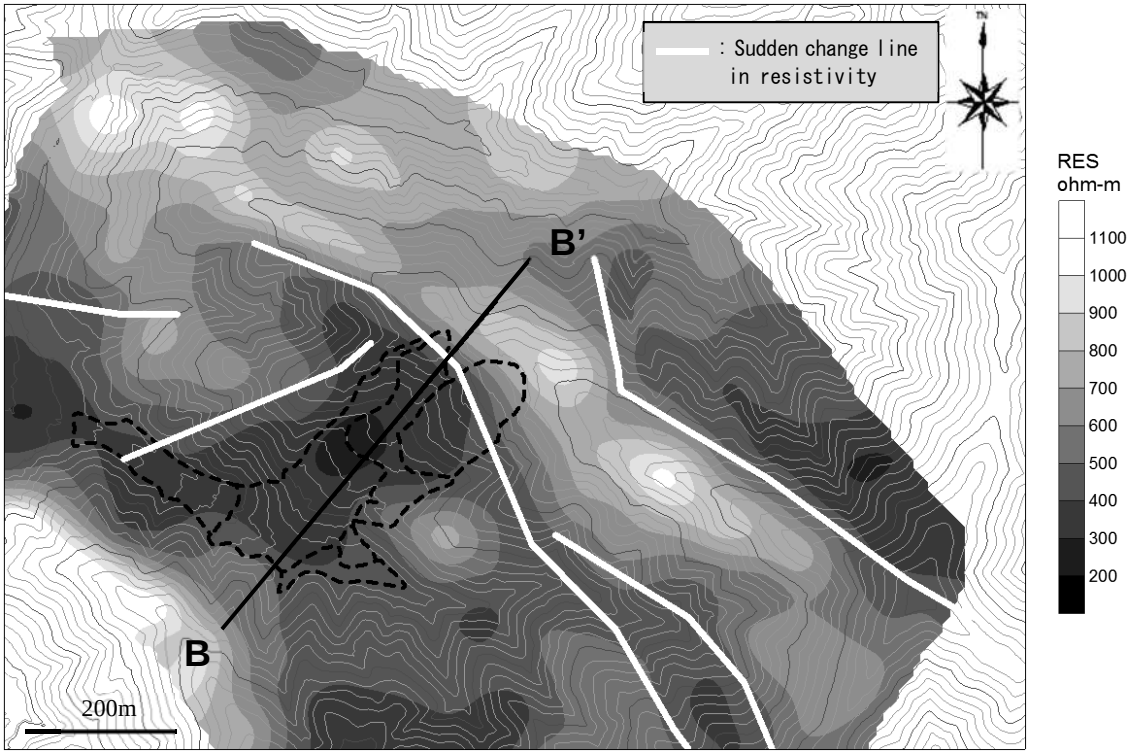

Fig.5 Resistivity distribution map view of the surface by airborne electromagnetic survey

The ridge extends in the northwest to southeast direction above the head scarp of the DCL. In the northeast side of the ridge, the specific flow rate is high. On a contrary, the specific flow rate is low in the southwest side of the ridge. Specific discharge of catchment area c-8 and c-9 larger than that of catchment area a-6, a-7 and a-8. In addition, the flow rate in the northeastern side of the ridge that extends southwest from the head of the landslide is larger than the values in southwest side (c-6 larger than c-5).

As a result of water permeability test that carried out using a drilling hole, a water hydraulic conductivity is $k = 1 \times 10^{-3} \sim 10^{-5}$cm/sec in sandstone dominant layer, and $k = 1 \times 10^{-4} \sim 10^{-6}$cm/sec in mudstone mixed rock layer.

The rock becomes fragile because zeolite of its kind generated by the hydrothermal alteration in addition to fracturing of rock layer by faults formed in the accretionary complex. It is confirmed the zeolite cloudy calcite veins, with quartz veins (Romontaito) pulse, have been developed along the F-1 fault in infacing dip layer. In addition, the gap tends to be generated along the vein because crystal structure gradually collapses missing crystal water with a repeated wet and dry condition above the groundwater level. Therefore, there is a possibility that the veins along the fault have become a predisposition for the looseness or formation of high- permeability zone.

F-1 fault along the ridge in the west-northwest to east-southeast direction restricts the hydrogeological structure. The predominant sandstone layer with high permeability is distributed thick on the ridges. And, those geological structures contribute to inflow of groundwater from the outside to DCL site. It is estimated that these factors may cause the occurrence of DCL.

3.4 Estimation of geological structure by airborne electromagnetic survey

The plan view of the surface portion of the resistivity by the airborne electromagnetic survey is shown in **Fig. 5** and the cross-sectional view in **Fig. 6**. Low resistivity zone distributed inside the landslide corresponds to the point of deposited sediment induced due to collapse. It is considered to represent condition of higher soil saturation. Since resistivity in the northeast side slope without collapse is relatively high in compared to the southwest side slope where the DCL occurred and the value becomes higher according to the depth

under the ground.

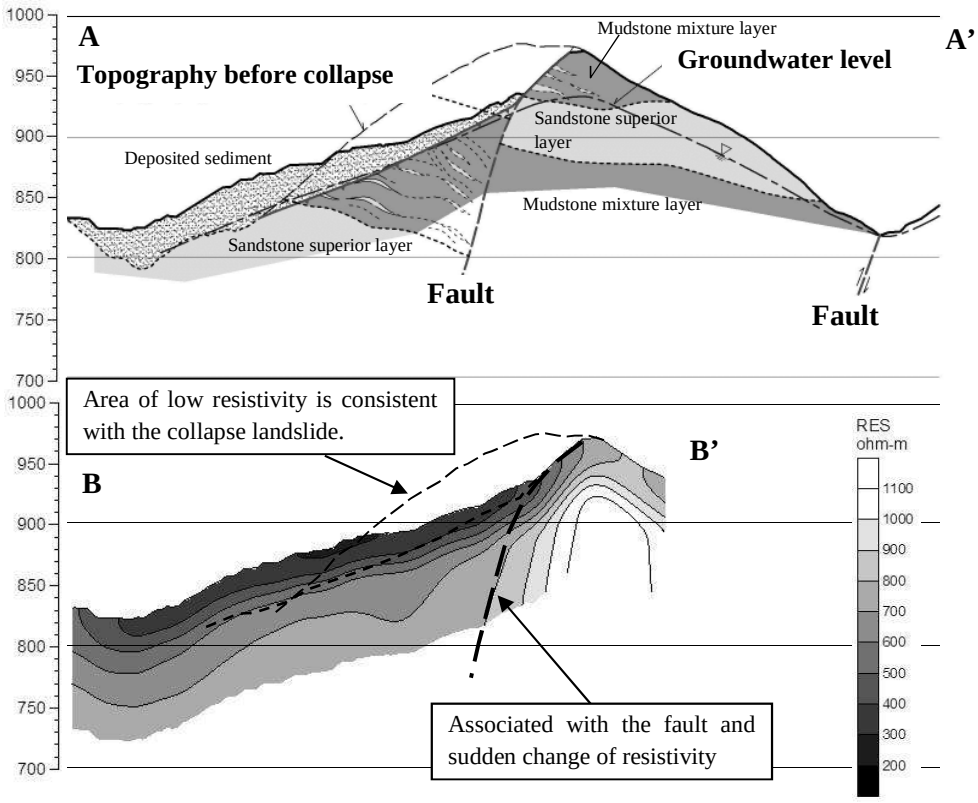

Fig.6 Geological cross-section of the landslide (upper) and resistivity cross-section

It is considered that the resistivity pattern represents the condition of the unweathered foundation rock.Sudden change in resistivity is found at the boundary between southwest slope where the collapse occurred and the northeast slope where the collapse did not occurred.

Similarly, the sudden change in resistivity is observed between the both sides of the ridge extending southeast to northwest of landslide. Sudden change of the specific resistivity is consistent with the position of the faults; F-1 fault in west-northwest to east-southeast direction faces along the head scarp of the collapse, and F-2 fault in the north-south direction that borders the west side of the collapse. It suggests that the existence of those faults is related to the sudden change of the resistivity.

4. CONCLUSION

Comparing the geological map and water discharge distribution map, a large difference can be seen in the specific water discharge in the upstream and downstream across the fault in the basin which is adjacent to the fault in the east-west direction and the fault in the north-south direction. The presence of a fault is considered to have an impact on the hydrogeological structure directly or indirectly. Accurate measurement of the flow rate is not performed in the collapsed slope because river water flows under the ground. However, there are paddy fields and traces in the area, so the flow rate is considered to be high.

Also, comparing the cross section of geological map and distribution of resistivity obtained by airborne electromagnetic survey, it can be seen that there is a relation between the existence of fault and sudden change of resistivity. Therefore, there is a possibility that the existence of fault can be estimated by the way mentioned above. Furthermore, by combining the extraction of the slope based on the topographical analysis such as creep slope

terrain interpretation and estimation of location of fault, it is possible to clarify slopes prone to undergo gravitational deformation and catch the groundwater from outside basin.

In order to estimate the geological structure regulating the landslides, we performed the airborne electromagnetic survey in the wide areas in addition to the geological survey. It is desired to conduct the more detailed hydrological observation and survey for surface water flow and groundwater level and investigate the mechanism of collapse in Kitamata district and other region. The accumulation of data for the measurements and the prediction of the occurrence of DCLs is very important issue to reduce those disasters.

REFERENCES

Archie, G. E.（1942）: The electrical resistivity log as an aid in determining some reservoir characteristics, Trans. A. I. M. E., 146, 54-67.

Chigira, M. and C Y Tsou, and Matsushi, Y. and Hiraishi, N. and Matuzawa, M. (2012): Site characteristics of deep-seated landslides induced by Typhoon 12–Analytical results by using high-resolution DEMs before and after the events –, Characterization, prediction, and management of deep-seated catastrophic landslides, pp. 24-34 (in Japanese with English abstract).

Sasahara, K. and Hiura, H. and Doshida, S. (2014): Geomorphological characteristics of the collapsed slopes due to Typhoon No. 14, 2005 at the upstream of the Monobe river, Kochi, Japan, Journal of Erosion Control Engineering, Vol. 66, No. 6, pp.40-49 (in Japanese with English abstract).

Takakura, S (2009): Influence of pore-water salinity and temperature on resistivity of clay-bearing rocks, The Society of Exploration Geophysicists of Japan, Vol. 62, No. 4, pp. 385-396 (in Japanese with English abstract).

Yokoyama, O. and Uchida, T. and Nakano, Y. and Ishiduka, T. and Kasai, M. and Suzuki, R (2012): Clarifying surface shape of mass rock creep revealed by using airborne LiDAR, Journal of Erosion Control Engineering, Vol. 64, No. 6, pp. 13-24 (in Japanese with English abstract).